

Development of Advanced Foams in Microgravity

Metallic and aqueous foams are challenging materials for both fundamental and applied research. They distinguish themselves from other materials by their very low density and, especially in the case of metallic foams, by high specific stiffness, good damping and high-energy absorption capability. They are therefore becoming increasingly popular for industrial applications. Driven by industry demand, efforts have been made in recent years to improve foam quality. Microgravity conditions are essential for further analysis and improvement of aqueous and metallic foams. Experimental devices for *in situ* and *ex situ* analysis were developed within this MAP project. Foam properties such as drainage, rupture events and foam density were analysed quantitatively, as well as the influence of external conditions like gas pressure and foaming gas. Hardness and wetting angles for different stabilising particles were compared; mica is proposed as a suitable candidate for aluminium foams. In the case of aqueous foams, surfactants and proteins are found to have a different microscopic origin of stabilisation. A monodisperse aqueous foam generator will be adapted for metallic foams. Foam stabilisation mechanisms and foam evolution simulations were performed. 2-D X-ray foam images were successfully simulated.

1. Introduction

Metallic foams have become increasingly important in recent years (Banhart & Weaire, 2002). Aqueous foams are better known systems, but differ from metallic foams. Both are complex systems whose creation and stabilisation are strongly influenced by gravity. This MAP project is concerned mainly

with the liquid stage as the foam structure evolves: the processes at this stage clearly influence the properties of the final solidified foam.

This European research initiative, with five academic partners, each specialised in a specific aspect of foam science, and supported by four very active and highly innovative companies, has already changed the pace of development and has brought fresh improvements in technology. A key objective is to supply knowledge to European industry that enables it to solve problems in the development and production of advanced foams.

The team's aim is to develop novel foams based on metals or other materials with improved properties. Microgravity provides an ideal experimental environment facilitating the study of wet foams, avoiding drainage and other gravitational phenomena (Weaire & Cox, 2004). A wet foam has a relatively high liquid content. The team wants to create, manipulate and compare such foams under normal and microgravity conditions, and study them *in situ* and in real-time. For this challenge, a modular experiment programme based on different experimental platforms (e.g. creating metallic foams by expanding precursors, by sparging gas through melts or creating and investigating columns of wet aqueous foams) was realised.

2. Metal Foam Analysis

2.1 *In Situ* Analysis of Metallic Foams

2.1.1 Evolution of Metallic Foams under Pressure

Here, the aim is to observe directly the details of evolution of a foaming system under surrounding pressure. This can be achieved using X-rays.

Report of the ESA MAP Team in Physical Sciences Development of Advanced Foams in Microgravity (MAP-99-075)

A compact microfocus X-ray source was used to monitor foam expansion kinetics while varying the temperature ramp and the TiH₂ blowing agent treatment (García-Moreno et al., 2005). New pressure furnaces were built and used to carry out high-pressure (~10 bar) and low-pressure (~0.001 bar) foaming experiments in an oxidising or inert atmosphere. The foam expansion F/F_0 can be calculated from the radioscopic images (F : area of cross section).

The gas pressure was found to influence foaming behaviour strongly. Under low pressures, high coalescence instabilities and large rising bubbles characterise the foaming process. Under high pressures, in addition to reduced expansion, an extremely small average cell size and high homogeneity was observed. Release from high pressure to normal pressure leads to an increased expansion (Fig. 1). Reversible expansion and compression after several pressure cycles were found, with a flexible cell wall structure. An additional expansion with high coalescence followed each cycle, increasing the maximal expansion from $F/F_0 \sim 1.5$ at 8 bar to $F/F_0 \sim 4$ at 1 bar.

The surrounding pressure plays an important role in microgravity experiments. These experimental findings have already provided rich information.

2.1.2 Examination of Wet Metal Foams Blown by External Gas Injection

With the aid of X-ray imaging, the behaviour of the foaming process under a variety of conditions can be investigated.

Foam evolution is strongly connected with the foaming gas used in the case of external gas injection. Oxidising gas, as air, results in a thick (100 nm) oxide skin on the cell wall

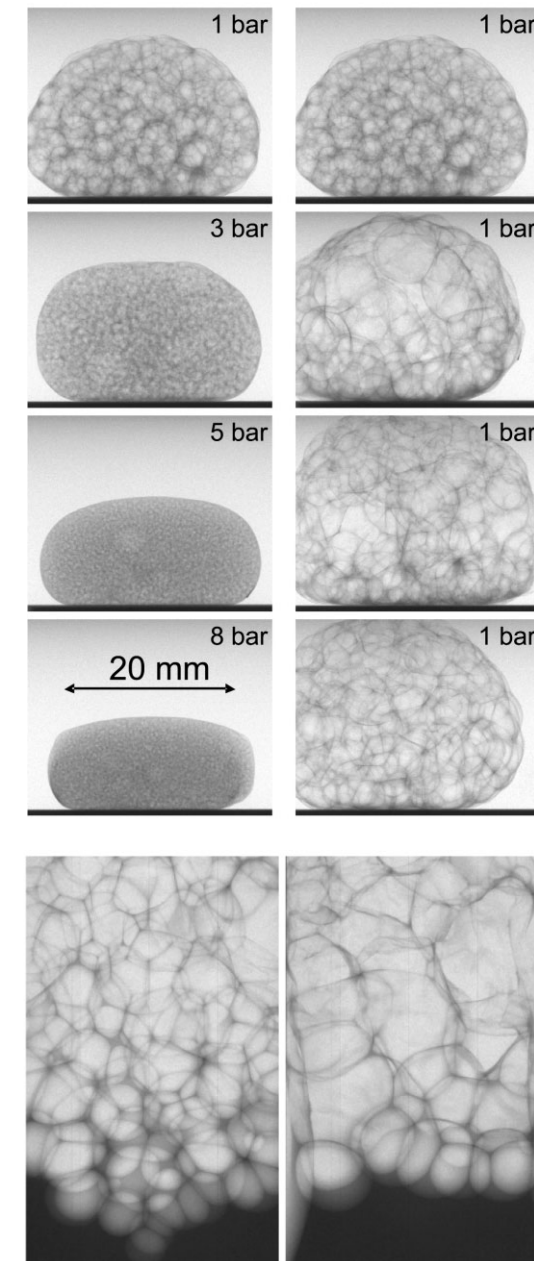


Fig. 1. Radioscopic images of Al99.7 samples foamed at different pressures (left) and after pressure release to 1 bar (right).

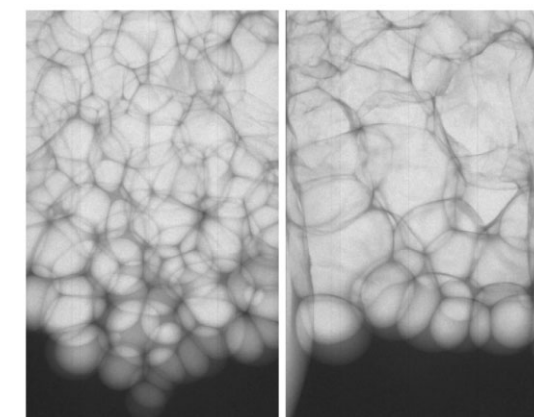
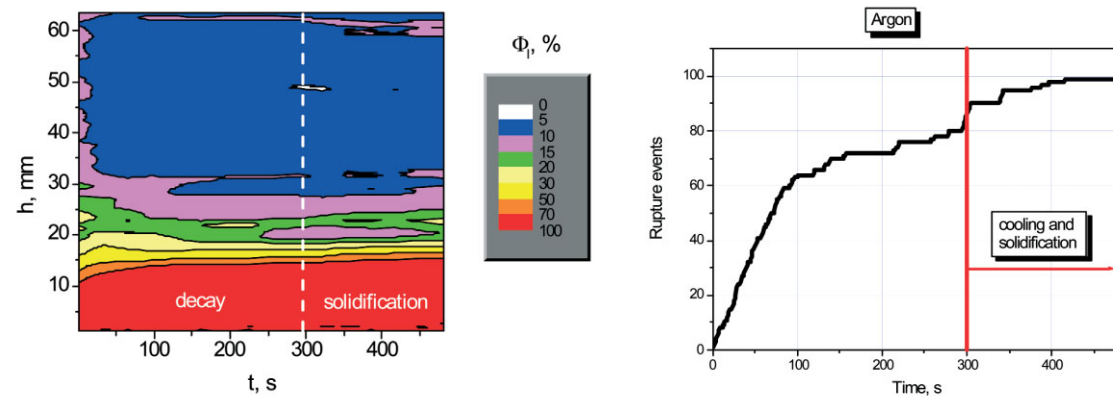


Fig. 2. X-ray images of foaming with Ar + 0.01% oxygen immediately after foam formation (left) and after 5 min holding in the liquid state and subsequent solidification (right).

surfaces, acting like a rigid stabilising layer. The role of oxidation in liquid metal foams is revealed by *ex situ* and *in situ* analysis (Babcsan et al., 2005).

The team was able to produce different foams with variable bubble sizes and volumes. X-ray images of the foam structures just after foaming, 5 min later and after solidification are shown in Fig. 2. Blowing Duralcan-type metal matrix composites

Fig. 3. Left: drainage diagram for sample in Fig. 2; colours represent density in % of the bulk metal. Right: accumulated rupture events during holding.



(AlSi7 + SiC), the drainage and the coalescence rate were quantitatively monitored. Significant drainage was found within the first 20 s of foam decay for argon-blown foam. In air-blown foam, drainage was hardly detectable. Isothermal holding for several minutes leads to coarsening and a slight degradation of uniformity in argon-blown foams, while air-blown foams remain almost unchanged even after 100 min. During solidification, foams shrink significantly (~10%) in both cases. This is more than for the liquid metal, but remember that >70% of the foam volume is air.

Foam evolutions were analysed quantitatively using the improved algorithms of image analysis software developed by the partners. Examples of the time-dependence of drainage and the numbers of accumulated rupture events in foams blown with argon (oxygen < 0.01%) are shown in Fig. 3.

2.2 Ex Situ Analysis of Metallic Foam Drainage

Two experimental setups were developed to investigate *ex situ* the drainage behaviour in liquid metallic foams. One is devoted to test experiments on the ground, while the second is a preliminary design for a future microgravity experiment on, for example, a parabolic flight.

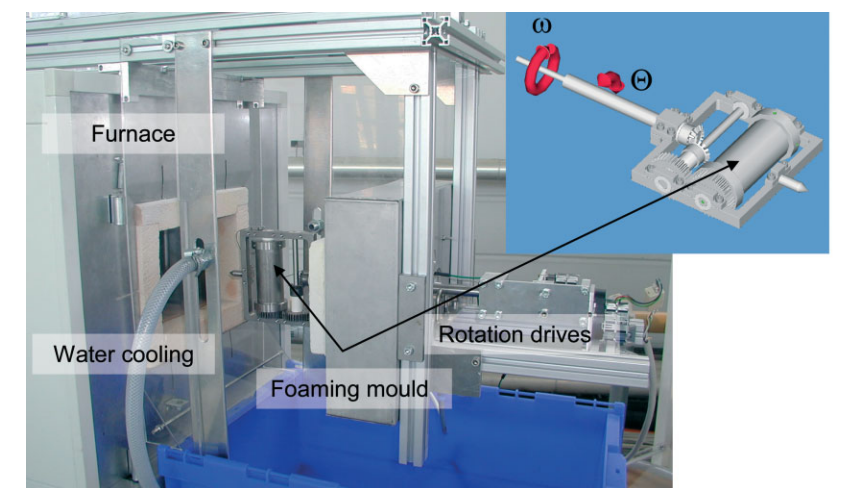
The first set-up (Fig. 4) indirectly observes the redistribution of the melt. After different drainage times, the foam is rapidly solidified and the density profile is determined by

separating the foam column into cylindrical segments.

Combined analyses of cross-sectional images and tomographic datasets of the foam samples provide information about the geometric properties (such as mean pore size and diameter of the Plateau borders) of the foam structure. In order to provide a reasonable comparison between experimental and numerical drainage results, the thermophysical properties, surface tension and viscosity of the liquid alloy have to be known. The viscosity of the precursor alloy was measured to be $\eta_{\text{precur}}(700^\circ\text{C}) = 1.7 \pm 0.1$ mPa.s. The value for the surface tension was taken from literature: at 700°C the surface tension of AlSi7 alloys is reported to be $\sigma_{\text{AlSi7}} = 0.8$ Nm. This information is used to give input parameters for the numerical solution of the Foam Drainage Equation (FDE).

The result of the experimental foam density profiles after different drainage times is shown in Fig. 5. The error-bars given for the experimental data represent the standard deviation of four measured drainage profiles. The small error bars indicate the good reproducibility of the experimental procedure. The numerical profiles were calculated using thermophysical and structural input parameters obtained from measurements and the literature. Owing to the rather low viscosity and the large area of the Plateau border channels, the drainage is rapid and reaches the equilibrium profile about an order of magnitude faster than in

Fig. 4. Furnace system for the observation of the drainage behaviour of metallic foams. The inset shows the cylindrical stainless steel foaming mould mounted on the 2-axis (ω, θ) sample manipulator.



the experiments. The increase of the bulk viscosity of the foam material by a factor of ~1.4 owing to the oxide content is thus insufficient to explain the slow drainage behaviour and relatively long stability of the foam. To account for the much slower process, a higher effective viscosity $\eta^* = \eta_{\text{AlSi7}} \cdot 10$ has to be assumed in order to reduce the simulated drainage rate.

2.3 Particle Stabilising Mechanisms and Novel Particles for Stabilisation

Foams produced commercially today are often produced via the Alcan route: bubbling of air or other gases through a liquid melt of aluminium. In order for the foam to be stable, fairly large amounts (typically 5-15wt%) of ceramic particles are added.

In many cases, silicon carbide is used as the stabilising particles. SiC is indeed a high surface energy material (2840 mJ/m², (Jiao et al., 1997)), and this will promote good wetting. However, this material has the drawback of being very hard. The hardness is a substantial drawback with respect to recyclability of the metal foams, as tools in the recycling machinery are damaged by abrasion through the SiC powder remaining in the material.

In order to get around this problem, a natural first step would be to use softer particles. Indeed, there are many inorganic materials with several-Moh hardness below that of stainless steel that would not do any harm to the machinery in aluminium recycling plants (Fig. 6). However, as hardness and surface energy are related to the internal bond strengths of a given material, the very soft materials also typically possess a low surface energy. In turn, this means that the very hard materials (having a high surface

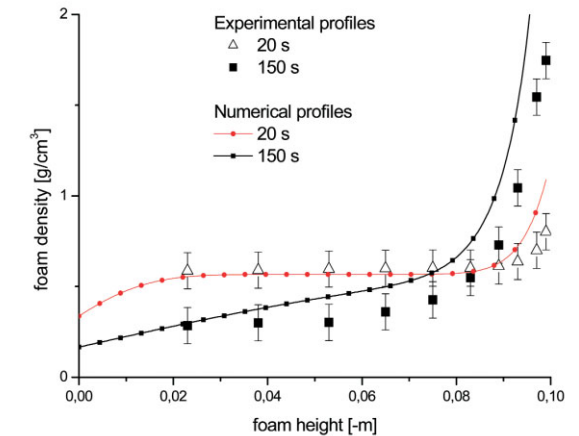


Fig. 5. Experimental drainage profiles (20 s and 150 s) of AlSi7 foams and the corresponding solutions of the FDE with using an initial, uniform, liquid content.

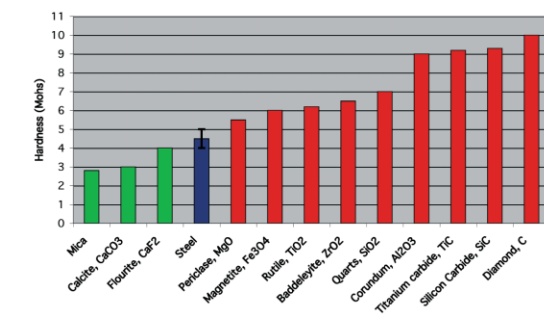
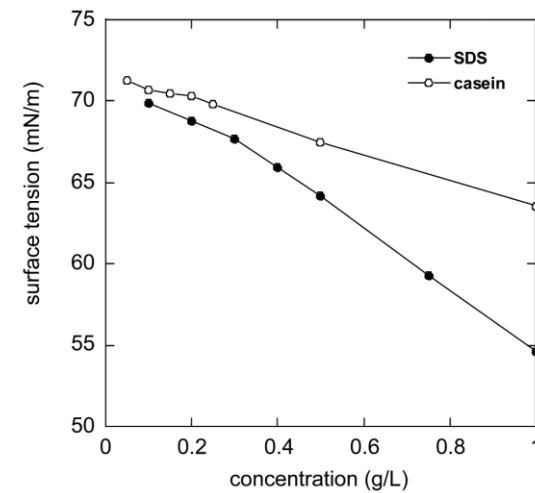


Fig. 6. Hardness of steel and a number of inorganic materials.

energy) will be the materials that are more readily wetted by a given liquid metal (such as molten aluminium).

In the case of the mineral mica, an interesting phenomenon related to surface energy is documented in the literature (Baily & Kay, 1967). It was found that the surface energy of mica is strongly related to the

Fig. 7. Surface tensions measured after 3 s, characteristic time of foam production, as a function of the SDS and casein concentration. The surface coverage is proportional to the slope of the curve.



amount of water vapour present above the mica surface. In a high-vacuum environment, surface energies of $\sim 5000 \text{ mJ/m}^2$ have been measured, whereas at ambient atmosphere conditions (50-60% relative humidity and room temperature) the surface energy has been measured as 220 mJ/m^2 . The large differences in surface energy are believed to stem from an adsorbed layer of water vapour being present at ambient conditions, thereby giving the low surface energy.

In the light of this, mica powder could be an interesting material for metal foam stabilisation, as it would certainly not have an adsorbed layer of water on its surface at, for example, 660°C in liquid aluminium. It would thereby have a high surface energy when mixed into liquid aluminium, which in turn would lead to good wetting and foam stability.

3. Aqueous Foams

3.1 Stabilisation by Surfactants and Proteins

The team made a detailed comparison between foams made with surfactants (SDS, sodium dodecylsulphate) and proteins (casein, milk protein, chosen in consultation with industrial partner Danone). It was found that the microscopic origins of foam stability are quite different for SDS and casein foams. (Saint-Jalmes et al., 2005) For surfactant foams, the repulsive interaction between the

adsorbed surface layers confers stability to the thin liquid films between air bubbles, and therefore stability to the foam. The surface coverage is an important parameter here, and it was determined by surface tension measurements (Fig. 7)

Figure 7 shows that, in the case of proteins, the surface tension remains close to that of water for short times, so the surface coverage is poor. When performing optical observations of the thin films, it was noticed that films with proteins were thick and full of seemingly gel-like aggregates (Fig. 8). The different colours (seen in Fig. 8 via interferometry) indicate the variations of thickness; the surface is clearly quite corrugated and deformed. This bumpy shape results from the adsorption of protein aggregates (of various morphologies); their interaction and confinement in the film provide a gel-like jammed behaviour.

The film stability threshold appears to correspond to the percolation of these aggregates in the film. With this type of stabilisation mechanism, which could be relevant for systems stabilised by other proteins or solid particles (as in metallic foams), the surface tension of the solutions cannot be linked as is usually done for surfactants to macroscopic foamability. However, for both casein and SDS, there are always clear correlations between the stability of a single thin film and that of the foam.

3.2 Monodisperse Foam Generation

Recently, the team has begun to improve the process of monodisperse foam formation, as currently practised in the leading technology of some companies. This produces highly homogeneous foam with almost the same

Fig. 8. Images of thin films obtained with the thin-film balance apparatus. Left: SDS film; right: casein film.

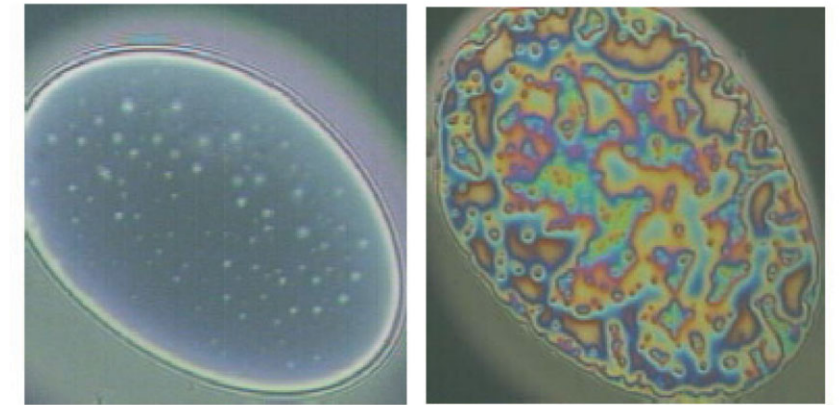
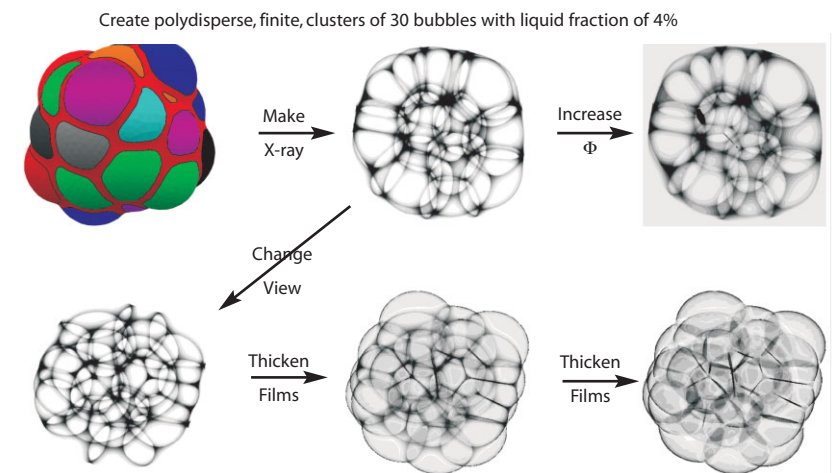


Fig. 9 (below right). Steps in simulating a 2-D X-ray image of a metallic foam.



bubble size and superior properties for engineering applications. The team has begun a study of bubble/droplet emission from nozzles, and is planning the adaptation of a new commercial instrument for metal foam formation in the laboratory. The previous work done on aqueous foams and the background on metallic foams are helpful in approaching the problem.

4. Simulation of Foam Phenomena

Interpretation, analysis and simulation were done of *in situ* metallic foam experiments performed in Section 2. The primary interest is in the role of drainage as a limiting factor in metal foam fabrication. Also being developed for the first time is a simulation of the effect of rotation. The recent experiments rotating the sample during foaming have provided a particularly informative range of data (Brunke et al., 2005). The importance of a temperature-dependent viscosity for the model was corroborated.

A further contribution is the interpretation of X-ray data, i.e. the mapping of a 3-D foam structure into 2-D. This was addressed using foam clusters with a finite liquid fraction as computed with the software Surface Evolver (Fig. 9). The next step is to compare the simulated and experimental images quantitatively, in order to be able to predict 3-D foam properties from their projected X-ray images. Compare Fig. 9 with Fig. 2 and Fig. 3.

5. Conclusions

The *in situ* observation of the density redistribution in metallic foams by means of X-ray radiography allows not only a precise determination of the drainage profiles during the whole process, but also provides

information about the evolution of the foam structure due to rupture events. A great influence of the gas pressure on the foaming behaviour was found. Under low pressures, high coalescence and rising big bubbles characterise the foams. Under high pressures, apart from a reduced expansion, small average cell size and high homogeneity was observed. Release from high pressure to normal pressure led to increased expansion. Also, reversible expansion and compression after several pressure cycles were found, with a flexible cell wall structure. An additional expansion with high coalescence followed each cycle, increasing the maximal expansion from $F/F_0 \sim 1.5$ at 8 bar to $F/F_0 \sim 4$ at 1 bar.

A first comparison between experimental results and numerical calculation shows that the standard FDE can principally be used to

describe drainage in metallic foams. But it becomes obvious that the difference in viscous behaviour, surface tension and density between liquid metals and water require an appropriate adjustment of the parameters used for the calculations.

It is concluded that the mineral mica might be useful for stabilising metal foams owing to its special feature of high surface energy in the absence of humidity (e.g. at 660°C in production of metal foams using the Alcan process and a dry blowing gas), and its low surface energy and hardness at ambient conditions owing to surface adsorption of water.

Many interesting differences were found between protein- and surfactant-stabilised aqueous foams. The differences seem to be closely related to the thicker films in the case of proteins, and might be similar in foams containing particles. A new method for the formation of monodisperse aqueous foams will be adapted for metallic foams.

The team's analysis of drainage data appears to validate the combined drainage and solidification model proposed previously, highlighting the importance of the inclusion of a temperature-based viscosity. The team is now able to simulate foams of given topology, ordered and disordered, with a range of liquid fractions, and extract a 2-D projected image that bears a close relationship to those from experiment.

References

Babcsán, N., Leitmeier, D., Degischer, H.D. & Banhart, J. (2005). The Role of Oxidation in Blowing Particle-Stabilised Aluminium Foams. *Adv. Eng. Mat.* **6**, 421-428.
Baily, A.I. & Kay, S.M. (1967). A Direct

Measurement of the Influence of Vapour, of Liquid and of Oriented Monolayers on the Interfacial Energy of Mica. *Proc. Roy. Soc. A* **301**, 47-56

Banhart, J. & Weaire, D. (2002). On the Road Again: Metal Foams Find Favor. *Physics Today*, July, 37-42.

Brunke, O., Hamann, A., Cox, S.J. & Odenbach, S. (2005). Experimental and Numerical Analysis of Free Drainage of Aluminium Metallic Foams; submitted to *J. Phys. Condens. Matter*.

García-Moreno, F., Babcsán, N. & Banhart, J. (2005). X-Ray Radioscopy of Liquid Metal Foams: Influence of Heating Profile. *Atmos. & Pressure, Colloids & Surfaces A*, **263**(1-3), 290-294.

Jiao, S., Jenkins, M.L. & Davidge, R.W. (1997). Interfacial Fracture Energy-Mechanical Behaviour Relationship in Al₂O₃/SiC and Al₂O₃/TiN Nanocomposites. *Acta Mater.* **45**(1), 149-156.

Saint-Jalmes, A., Ferraz, H., Peugeot, M.L. & Langevin, D. (2005). Differences between Protein and Surfactant Foams: Microscopic Properties, Stability and Coarsening. *Colloids & Surfaces A*, **263**(1-3), 219-225.

Weaire, D. & Cox, S.J. (2004). Foams, Films and Surfaces in Microgravity. *Proc. XXI Internat. Cong. of Theoretical and Applied Mechanics Warsaw, Poland*; in Press.

MAP Team Members*Academic Partners*

Dr. Francisco García-Moreno
 Technical University Berlin – Materials
 Science PN 2-3, Hardenbergstr. 36,
 D-10623 Berlin, Germany.
 Tel: +49 30 8062 2761
 Fax: +49 30 8062 3059
 Email: garcia-moreno@hmi.de

Dr. Norbert Babcsan
 Technical University Berlin – Materials
 Science PN 2-3, Hardenbergstr. 36,
 D-10623 Berlin, Germany.
 Tel: +49 30 8062 2761
 Fax: +49 30 8062 3059
 Email: babcsan@hmi.de

Prof. Dr. John Banhart
 Technical University Berlin – Materials
 Science PN 2-3, Hardenbergstr. 36,
 D-10623 Berlin, Germany.
 Tel: +49 30 8062 2710
 Fax: +49 30 8062 3059
 Email: banhart@hmi.de

Dr. Martin Andersson
 Institute for Surface Chemistry, Drottning
 Kristinas väg 45, S-11486 Stockholm,
 Sweden.
 Tel: +46 8 50106025
 Fax: +46 8 208998
 Email: martin.andersson@surfchem.kth.se

Prof. Dr. Robert J. Pugh
 Institute for Surface Chemistry, Drottning
 Kristinas väg 45, S-11486 Stockholm,
 Sweden.
 Tel: +46 8 50106076
 Fax: +46 8 208998
 Email: bob.pugh@surfchem.kth.se

Prof. Dr. Bengt Kronberg
 Institute for Surface Chemistry, Drottning
 Kristinas väg 45, S-11486 Stockholm,
 Sweden.
 Tel: +46 8 50106057
 Fax: +46 8 208998
 Email: bengt.kronberg@surfchem.kth.se

Dr. Arnaud Saint -Jalmes
 Laboratoire de Physique des Solides - Université
 Paris Sud, Bâtiment 510, F-91405 Orsay,
 France.
 Tel: +33 169 156960
 Fax +33 169 156086
 Email: saint-jalmes@lps.u-psud.fr

Sébastien Marze
 Laboratoire de Physique des Solides - Université
 Paris Sud, Bâtiment 510, F-91405 Orsay,
 France.
 Tel: +33 169 155388
 Fax +33 169 156086
 Email: marze@lps.u-psud.fr

Dr. Dominique Langevin
 Laboratoire de Physique des Solides - Université
 Paris Sud, Bâtiment 510, F-91405 Orsay,
 France.
 Tel: +33 169 155351
 Fax +33 -169 -156086
 Email: langevin@lps.u-psud.fr

Dr. Oliver Brunke
 Centre of Applied Space Technology and
 Microgravity, Am Fallturm, D-28359 Bremen,
 Germany.
 Tel: +49 421 218 4844
 Fax: +49 421 218 2521
 Email: brunke@zarm.uni-bremen.de

Prof. Dr. Stefan Odenbach
 Centre of Applied Space Technology and
 Microgravity, Am Fallturm,
 D-28359 Bremen, Germany.
 Tel: +49 421 218 4785
 Fax: +49 421 218 2521
 Email: odenbach@zarm.uni-bremen.de

Dr. Simon Cox
 Institute of Mathematical and Physical
 Sciences, University of Wales Aberystwyth,
 SY23 3BZ, UK.
 Tel: +44 1970 622764
 Fax: +44 1970 622777
 Email: foams@aber.ac.uk

Dr. Stefan Hutzler
 Physics Department, Trinity College Dublin,
 Dublin 2, Ireland.
 Tel: +353 1 608 1676
 Fax: +353 1 671 1759
 Email: Stefan.hutzler@tcd.ie

Dr. Wiebke Drenckhan
 Physics Department, Trinity College Dublin,
 Dublin 2, Ireland.
 Tel: +353 1 608 2157
 Fax: +353 1 671 1759
 Email: wiebke.drenckhan@tcd.ie

Prof. Dr. Denis Weaire
 Physics Department, Trinity College Dublin,
 Dublin 2, Ireland.
 Tel: +353 1 608 1055
 Fax: +353 1 671 1759
 Email: dweaire@tcd.ie

Industrial Partners

Dipl.-Ing. Frank Baumgärtner
 Schunk Sintermetalltechnik GmbH, Postfach
 10 09 51, D-35339 Gießen, Germany.
 Tel: +49 641 608 1420
 Fax: +49 641 608 1734
 Email: baumgaertner@schunk-group.com

Dr. Wolfgang Seeliger
 Advanced Lightweight Materials GmbH,
 D-66123 Saarbrücken, Germany.
 Tel: +49 681 9382 841
 Fax: +49 681 9382 842
 Email: wolfgang.seeliger@t-online.de

Dr. Jean-François Argillier
 Institut Français du Pétrole, 4 avenue de Bois
 Préau, F-92502 Rueil Malmaison, France.
 Tel: +33 1 47 52 67 66
 Fax +33 1 47 52 70 58
 Email: J-Francois.ARGILLIER@ifp.fr

Dipl.-Ing. Dieter Lange
 Innovativer Werkstoffeinsatz, Mühlenstr. 1,
 D-17489 Greifswald, Germany.
 Tel: +49 3834 855530
 Email: iwegreifswald@aol.com